Electromagnetic-to-seismic conversion: A new direct hydrocarbon indicator

A. H. Thompson, John R. Sumner, and Scott C. Hornbostel, ExxonMobil Upstream Research Company, Houston, USA

We present novel methods that directly detect hydrocarbons based on conversions between electromagnetic and seismic energy. We first introduce the subject and then discuss the experimental methods in three field tests. Next, we present the results of the tests and then end with a few model results and thoughts about future applications.

Thompson and Gist (1993) detected seismic-to-electromagnetic (SE) conversions from 300-m-deep gas sands. Seismic waves, generated at the surface, convert to electromagnetic waves at gas sands; grounded dipole electrodes detect the EM response. These were the first data to document that a seismic signal from the surface generates a detectible electromagnetic response from reservoir units at significant depth. Their research also detected the inverse process, electromagnetic-to-seismic (ES) conversion.

ES and SE conversions are potentially powerful tools for identifying hydrocarbons and for reservoir delineation. These conversions give information about the electrical properties of hydrocarbon accumulations with seismic resolution. Unlike electromagnetic methods, ES/SE electrokinetic conversions are largest where the resistivity is high *and* where pore spaces contain mobile fluids. Resistive but impermeable bodies do not create electrokinetic conversions.

We recently discovered ES conversions that are second order in frequency. At a hydrocarbon accumulation, an electromagnetic wave at frequency f converts to a seismic wave at frequency $2f$. Harmonic generation offers the potential to enhance spatial resolution.

There are several advances in our understanding of electrokinetic coupling of seismic and electromagnetic energies since 1993. Pride (1994) developed the governing equations that couple the two energies; the distortion of pore-surface dipolar structures creates an electric field in an applied pressure gradient or creates a pressure gradient in an applied electric field.

Simultaneously with theory development, ExxonMobil's Upstream Research Company and Corporate Strategic Research Laboratory advanced the application of ES and SE coupling to hydrocarbon exploration and production. ExxonMobil presented four papers on this topic at the 2005 SEG Annual Meeting. White (2005) published an asymptotic separation of the Pride governing equations that enables rapid numerical solutions. Additional publications on numerical solutions in layered-earth geometries, laboratory studies of electrokinetics, and mechanisms for ES couplings are in press.

A significant change in direction over the last 15 years is the recognition that ES coupling is easier to implement than SE and yields conversions of higher energy efficiency. The ES data reported here demonstrate conversions at gas sands 1000 m deep and carbonate reservoirs 1500 m deep. In favorable locations on land, and with further developments of the technology, ES conversions may be detectable from greater depths. We find that electromagnetic attenuation is important but is not the limiting factor in generating signal from depths of several thousand meters. Other factors, such as near-surface noise coherent with the source, may be a concern. We have not tested offshore applications, but they should be feasible.

We find good ES signal-to-noise (S/N) ratios in basins with resistivities greater than a few ohm-meters. High S/N ratios are possible because ES data collection and processing can yield seismic sensitivities several orders of magnitude greater than is typically expected in seismology. Additionally, ES conversion amplitudes may be much larger than predicted for one interface because heterogeneity and layering can substantially increase ES amplitudes.

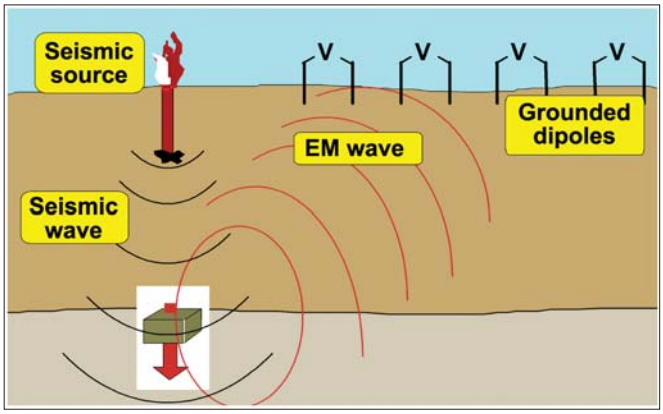

Figure 1. *Schematic of seismoelectric (SE) conversion. The seismic wave, generated at the surface, creates a pressure gradient at a rock interface where distorted dipolar structures on pore surfaces produce an electric field. The time-varying electric field propagates to the surface where grounded dipole electrodes detect its arrival.*

Description of ES and SE conversions. Figure 1 schematically displays the field-scale conversion of seismic waves to electromagnetic waves, or seismoelectric (SE) coupling.

At a contrast in acoustic impedance, a portion of the incident seismic energy creates a pressure gradient in the pore space that displaces dipolar layers on pore surfaces. Pore-surface dipoles, characterized by fixed charges on the grains and opposite-sign mobile ions in solution, are present when the rock grains are water wet and the pores contain some saline solution. Relative displacement of these fixed and mobile charges creates a macroscopic electric field when averaged over the pore space. This field has the same frequency as the incident seismic wave and propagates away from the acoustic-impedance interface. Grounded-electrode dipoles detect this diffusive electromagnetic propagation at the Earth's surface.

Three conditions favor large SE amplitudes—contrast in acoustic impedance, permeable pore space, and high resistivity pore fluids. Of these three, the contrast in acoustic impedance may be the weakest determinant of SE amplitude. Seismic reflection coefficients are small, often less than 1%. Most of the incident seismic energy propagates through the target interface unperturbed. Small seismic reflection coefficients favor using the inverse process, electroseismic conversion.

Figure 2 schematically displays the field-scale conversion of electromagnetic waves to seismic waves, or (ES) coupling.

Electrodes are on or near the surface of the Earth. The spacing of the electrodes is similar to the depth of the target. A potential difference applied to these electrodes drives a current into the subsurface. At a contrast in electrical properties, the vertical component of the electric field is dis-

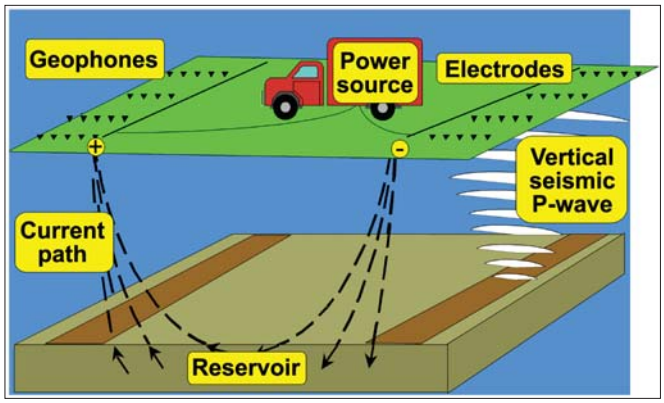

Figure 2. *Schematic of electroseismic (ES) conversion. An electric field applied to the electrodes drives current to the reservoir where the largest vertical current converts to the largest, vertically propagating P-wave. Digital accelerometers detect its arrival.*

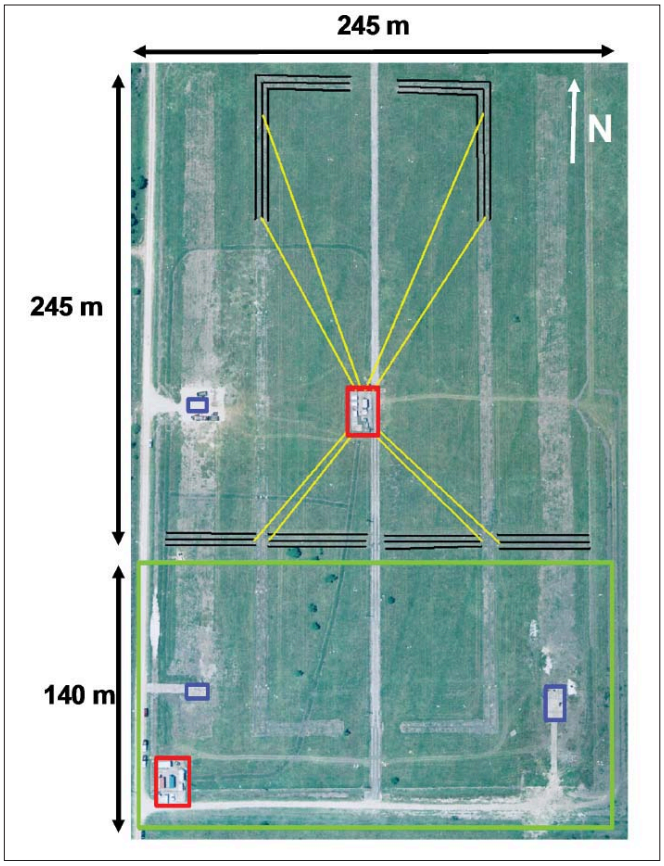

Figure 3. *Aerial photo of a Gulf of Mexico coastal site in Texas. The blue boxes are well locations, the yellow lines are bus wires, the black lines are electrodes, the red box in the lower left is the doghouse site, and the red box in the center is the location of the power source. The green box outlines the geophone array of 10 × 18 stations.*

continuous. The resulting gradient in field creates a local displacement of the pore-surface dipole layers. The charge displacement creates local, relative flow between the pore and grain spaces or induces a pressure gradient in the rock.

Contrasts in electrical conductivity at reservoir boundaries are large. The resulting electric field gradients strongly couple to pore-level charge displacement so that a relatively large fraction of the incident electromagnetic energy converts to pore-pressure gradients. By "relatively large" we mean relative to the SE conversion case. This high-efficiency of ES conversion is the principal reason to choose ES over SE methods. In addition, the convenience of an electromagnetic source and the absence of electromagnetic interference in digital accelerometers also favor ES over SE.

An exploding reflector is a good model for the seismic response to an electrical stimulus. The seismic literature discusses the exploding reflector in detail.

Digital accelerometers detect the ES response above the area of maximum vertical electric field where the maximum seismic amplitude reaches the surface. Digital accelerometers are required to achieve the low electromagnetic pickup required to extract the small ES signals from the background noise.

Many mechanisms create ES and SE coupling. An applied electric field interacts with any internal field in a rock to create ES coupling. For example, an applied field can induce second-order coupling through electrostriction. Likewise, an applied pressure gradient can change the volume of rock containing an internal field and create an SE response. Generally, the literature ignores these mechanisms and discusses only electrokinetic coupling.

All of the coupling mechanisms we have studied are sensitive to rock properties that make them potentially useful for hydrocarbon exploration—contrast in acoustic impedance; a permeable pore space; and resistive pore-filling fluids. Contrasts in electrical properties and macroscopic internal electric fields dominate the ES amplitudes.

Field methods. This paper concentrates on ES conversion. The field methods implement the concepts expressed in Figure 2. We discuss two examples and refer to a third published elsewhere.

Example 1—Gulf coast gas sands. Figure 3 shows the electrode and geophone layout for a survey of 100–500 m deep gas sands located in the coastal Gulf of Mexico, Texas. The electrodes are wires buried in trenches approximately 0.3 m deep. The power source is capable of producing 350 kW of power as a coded waveform.

For small surveys of this type, where the electrode length and separation are each a few hundred meters, power injection is limited by heating near the electrodes. To avoid heating effects, the current is limited to one ampere per meter of electrode length. Alternatively, surrounding the electrode with moist conducting clay achieves higher current densities.

At all test sites, an on-site weather station monitored conditions. Weather changes alter the ground resistance and the performance of the source. Lightning may cause a hazard with high-power equipment. Wind degrades the S/N ratio of the geophone array. Weather conditions can influence the test performance.

Inhomogeneities in the conductivity of the near surface may distort the electric fields at depth and confuse data interpretation. We collected three-component magnetic field and two-component electric field data on a 3-m grid around the operating electrodes. Comparisons of measured fields with the predictions of numerical simulations and independent measurements of the near-surface electrical conductivity were in good agreement. Complete interpretation of the details of ES data may require folding in the large-scale parts of this overprint. Small-scale variations in current will heal out before the current reaches the target.

This site was characterized by well logs, electrical surveys, and seismology before beginning ES data collection. The ES tests confirmed the existence of the gas sands.

Example 2—carbonate reservoirs in west Texas. The test at the carbonate site in west Texas was similar to the Gulf coast site but on a much larger scale. The target depth was greater than 1400 m. The power source was a maximum of three

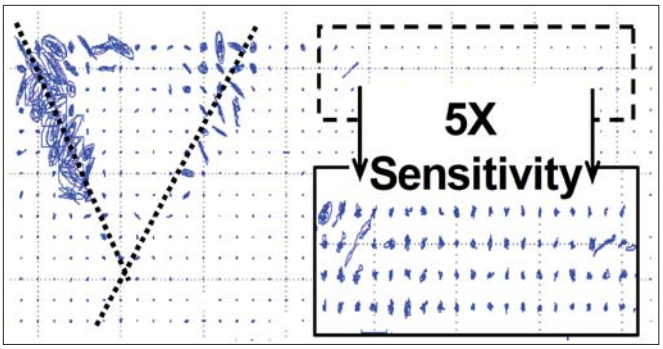

Figure 4. *Hodogram of horizontal digital accelerometer components at the west Texas site. Surface waves, generated where the electrode crosses a buried pipe, caused the high-amplitude events on the left. The expanded sensitivity on the right shows that the electrodes themselves generate electroseismic coupling. The data are nonlinear ES conversions. The electrode is located along the top of the display.*

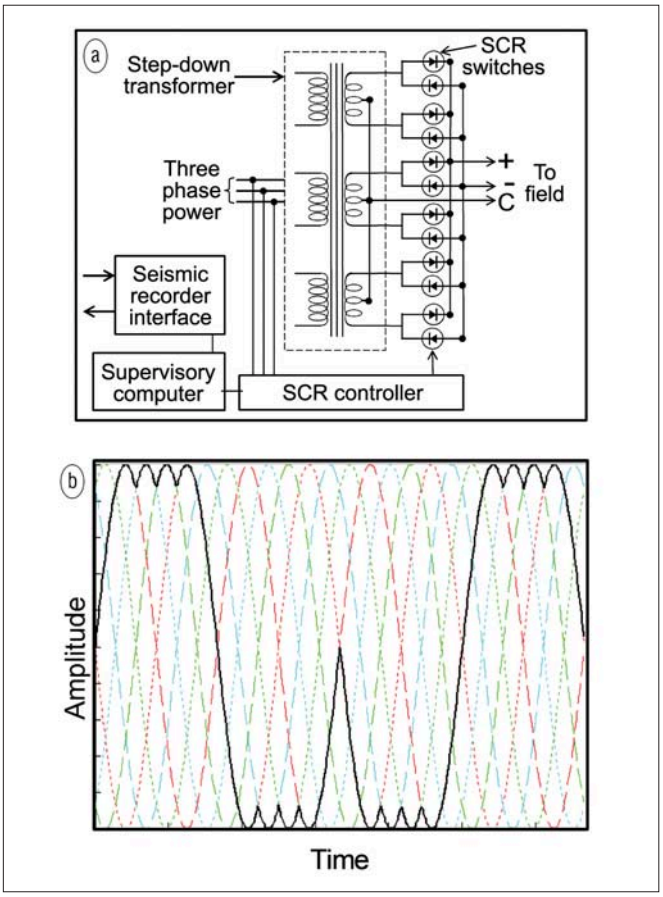

Figure 5. *The top figure is a block diagram of a power waveform synthesizer or PWS, which combines portions of a three-phase power line to form a specified waveform. The bottom figure illustrates a coded waveform where each of the three phases can have one of two polarities. The black curve is the envelope of selected portions of phases in the waveform.*

megawatts. The electrode configuration covered an area approximately 2 × 2 km.

In larger-scale surveys, where the electrodes may be kilometers in size, circuit inductance limits the current input. There are several contributions to the inductance. The inductance of the large current loop flowing though the ground down to the target is a principal concern. This inductance can limit current at frequencies above a few Hz to less than one ampere per meter of electrode wire. Generally, source design changes may compensate for this inductance.

Three-component, digital accelerometers discriminate between surface waves from noise sources and the vertical-traveling P-wave signal. Figure 4 is a hodogram plot of the horizontal components of the data from west Texas. Noise sources originate at the electrodes and field infrastructure. Interaction of the source EM field with pipelines crossing beneath the electrodes caused some noise. The electrodes directly generated electroseismic conversions observed in the hodograms.

We have identified ways to suppress source noise from the electrodes and infrastructure noise associated with pipelines and fences. Source noise limits the data collected, so advances in source-noise suppression may significantly improve the overall S/N and depth penetration.

Example 3—gas sands in Alberta, Canada. Thompson et al. (2007) collected data over 1000 m deep gas sands in Alberta, Canada. That work succeeded in detecting the 1000 m target. In those tests, we improved electrodes and equipment deployment. We used stake electrodes driven to a depth of 3 m. Installation and pickup of these electrodes, even under harsh conditions, is as fast as laying out seismic equipment.

Signal generation and processing. The seismic amplitude from an ES conversion may be many orders of magnitude smaller than the amplitudes typically encountered in seismology. Several factors combine to enable detection of these small signals.

The electromagnetic source permits collecting data continuously in time. The EM source can drive current into the ground for greater than 95% of the clock time. Dynamite and vibrator sources are also less efficient than an electrical source in terms of useful energy injected into the ground for each unit of fuel used.

The high efficiency of an electrical source, and the absence of moving parts in the signal generator, make it feasible to collect many repetitions of the source waveform. In a typical field test, a stack from one location contains 100–1000 repetitions of a 30-s waveform.

After many repetitions in a stack, source noise dominates the remaining noise. Noise spreads generated with vibrators placed along the source electrodes, horizontal seismic amplitudes associated with infrastructure noise sources as shown in Figure 4, and refined electrode configurations identify noise. Signal processing discriminates against these noises.

Taking full advantage of the data collection requires optimal source waveforms. Figure 5 illustrates an efficient means for constructing coded waveforms (Hornbostel and Thompson, 2007). Coded waveforms, generally variations on binary-coded waveforms, are constructed from portions of a three-phase power-line. Optimal sequences for ES applications ensure that side-lobes produced by correlation of the source and signal do not interfere with the signal in the time domain.

Figure 5 illustrates how the portions of the three-phase source combine to construct a sequence with a frequency lower than the power line frequency. The challenge in constructing the electromagnetic source is that the current levels are thousands of amperes and the switching time resolution is tens to hundreds of microseconds. The power waveform synthesizer (PWS) (Figure 5) is designed to perform the rapid switching.

Figure 5 shows a block diagram for a PWS. A transformer steps down the high-voltage power source to a few hundred volts. Silicon-controlled rectifiers (SCR) switch between phases. SCR controllers switch each SCR while a supervisory computer programs the coded waveform and interfaces with the seismic data acquisition system.

Each PWS handles 350 kW. Series or parallel combina-

Figure 6. PWS field installation in west Texas. Each PWS weighs 3000 kg and produces 350 kW of coded-waveform power at 120 V. They are truck transportable and rest on vibration-isolation skids. The wires from each PWS are 4/0 welder's cable connected to the electrodes.

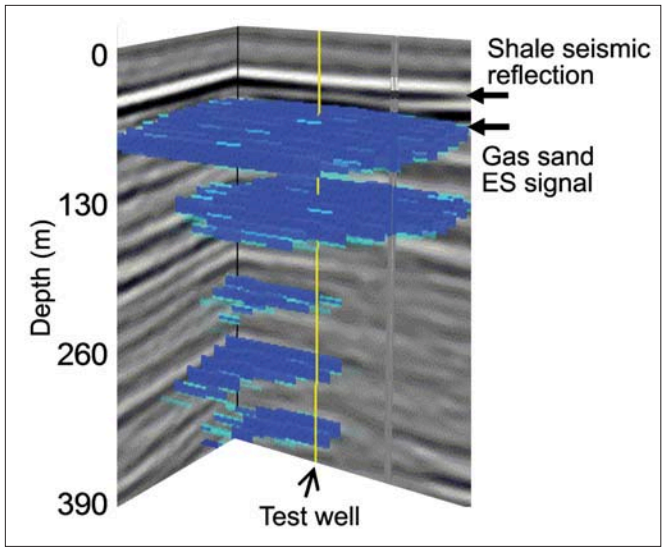

Figure 7. ES gas-sand data from the Gulf coast. The background is two sections of a 3D seismic survey. The blue regions are the areas of highest ES amplitude. Low amplitude ES signals are transparent. The shapes and depths of the ES signals are the ones expected for the applied electric fields at the known gas sand depths. A test well, as indicated, confirmed the location of the gas sands.

tions change the power supplied to the ground. Each PWS weighs 3000 kg and is skid-mounted and truck-transportable. Figure 6 shows a PWS installation. The wires from each PWS are 4/0 welder's cable going to the field electrodes. Vibration-isolation prevents coupling transformer parasitic vibrations to the ground. The processed signal is so small that these parasitic vibrations create significant source noise when a PWS is close to an electrode.

Health, safety, and environment. Electroseismic surveying requires higher electrical power levels than typically encountered in electromagnetic surveying. We gave careful attention to the potential electrical hazards.

The electrodes and the ground are in good electrical contact so they are at the same potential. The potential difference between a person or an animal standing near the electrode and the electrode itself is small. This "touch potential" is the voltage difference of concern with regard to electrocution hazard. The electrocution hazards are minimal with insulated bus wires.

The voltages are a few hundred volts applied over kilometers of distance. Such potential differences are similar to natural potentials generated by magnetic storms (Lanzerotti and Gregori, 1986).

The magnetic fields around the bus and electrode wires pose a risk for people with pacemakers and cochlear implants. Warnings, barriers, and monitoring equipment mitigate exposure to magnetic fields.

Equipment explosions are the most significant risk. High-power contactors may fail, create arcing, and an explosion hazard. We used fast fuses that limit currents to a level that will not cause an equipment explosion.

Results from Gulf coast gas sands. Figure 7 is a three-dimensional perspective image of ES data collected with the electrodes of Figure 3.

The background of the figure is orthogonal sections of 3D seismic data. The blue areas are high-amplitude ES events. The S/N ratio is high for these gas sands. Well logs confirm that these high-amplitude ES volumes are associated with gas sands. The high-amplitude seismic reflection just above the shallow ES data is associated with a shale lying 5 m above the gas sand while the ES data originate at the depth of the gas. The blue areas decrease in size at depth because the vertical electric field generated by the electrodes decreases with depth in this fashion, as shown in Figure 2.

The well, indicated in the figure and drilled to confirm the ES interpretation, is 350 m deep. Logging that well supported the ES results. The ES survey detected an additional signal at 500 m, deeper than the well. Although unconfirmed, the 500-m deep signal has the spatial dependence expected for an ES gas response from that depth. We conclude that this experiment, set up to detect gas sands to a depth of 130 m, successfully detected gas sands to a depth of 350 m and possibly 500 m, with good S/N ratio.

Many complementary data sets confirmed the interpretation of ES conversions from the gas sands. These include well logs, downhole hydrophones, electrical surveys, and electrode characterization measurements.

The data collection in this Gulf coast sand abundantly illustrated the power of ES detection of gas sands. The data show the power of resolving fine structure using ES by resolving the 5-m difference between the shale and gas sand.

Results from west Texas carbonate reservoirs, high-order rectifying ES, a new electroseismic conversion phenomenon. Figure 8 is a 3D perspective of ES data from the top of a carbonate oil reservoir at a depth of 1500 m. The backdrop is a seismic traverse through the reservoir section. There are three wells shown in Figure 8. Hydrophone and logging data characterize the formation and confirm that ES signals originate at depth. The wire frame is the top of the producing interval. The ES signal ties well with seismic studies from the same interval. The red pattern is the region of highest ES amplitude.

The data of Figure 8 are qualitatively different from any ES or SE data collected before. We were unable to separate first-order ES responses from source-generated noise. Instead, we found that there exist higher harmonics of the source ES signal. The data of Figure 8 are the result of processing the signal for an ES response at double the source frequency. Preliminary analysis shows that the ES-seismic wavelet contains other, higher harmonics, and the source waveform may be rectified. Figure 9 illustrates this rectification as recorded in a well.

The well data of Figure 9 are upward-propagating tube

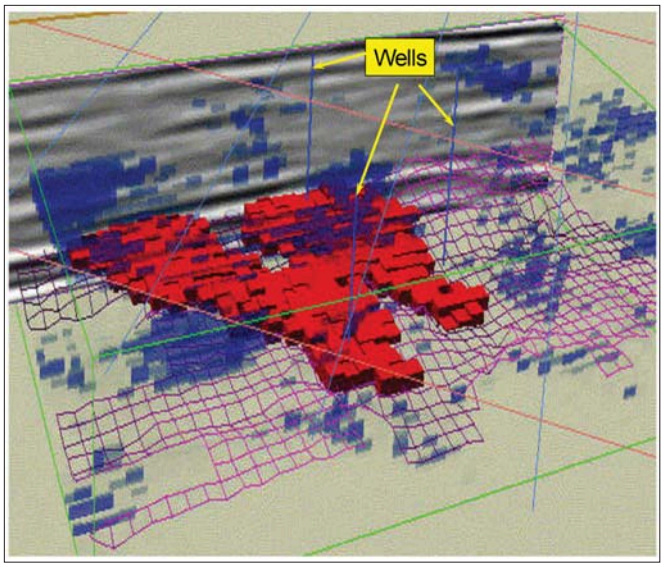

Figure 8. *ES carbonate oil-reservoir data from west Texas. The wire frame is the ES data that delineate the top of the reservoir. The red region is the region of highest ES amplitude. Data from the indicated wells support the ES data interpretation. The structure of the high-amplitude ES data is consistent with known reservoir properties, including the existence of a fault on the right of the figure that terminates the reservoir. The depth is 1500 m, and the image lateral dimensions are approximately 500 × 1000 m. The backdrop is a seismic traverse.*

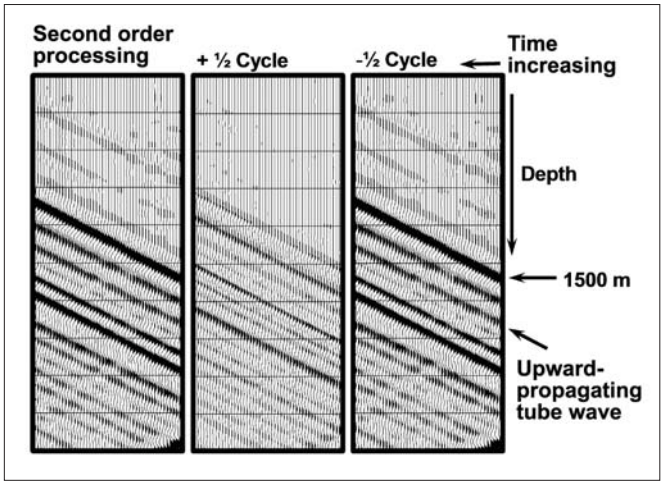

Figure 9. *Well data showing rectification of the ES signal from west Texas. The data are upward propagating tube wave data from reservoirs below 1500 m deep. The positive and negative portions of the ES wavelets have different amplitudes, as expected for a rectified signal.*

waves measured with downhole hydrophones. The tube waves originate at the reservoir intervals. The first panel shows the full wavelet of the second-order processing. The second panel shows the +½ cycle of the wavelet while the third panel shows the -½ cycle. The negative half cycle has higher amplitude than the positive half cycle. The asymmetry in the waveform is a signature of rectification of the wavelet and of the presence of higher-order harmonics of the source. The source waveform is not a simple sine wave, and the processing has permitted the higher-order harmonics to pass through while efficiently rejecting the fundamental frequencies of the source waveform.

We detect the harmonic ES signal even though it is smaller than the anticipated first-order signal. This is because most of the source-related noise is first order, and second-order processing removes the first-order component. Many source repetitions suppress the random noise. Random noise has not been a problem in our experience.

Several mechanisms yield higher-order conversions. These include electrostriction. The data are not consistent with an electrostriction mechanism because electrostriction should yield only squaring of the fundamental, not odd harmonics. Rectification may occur wherever the applied field modulates an internal electric field. Thompson (personal communication) has proposed that polarization of the spontaneous potentials at rock boundaries explains the observed properties of nonlinear ES conversion.

Additional work is required to verify the second order, rectifying conversions, and to identify their origin.

Modeling the linear ES response. Over the last eight years, ExxonMobil developed numerical modeling capability for the linear response in both layered and 3D structures. ES modeling involves three steps. First is the propagation of the diffusive EM wave down to the target. Second is the local coupling between the EM and seismic response at the target. Third is the propagation of the seismic wave back to the surface. In his asymptotic separation of the ES equations, White (2005) showed that the propagations down and back are separable from the coupling part of the problem. White's formalism should handle any seismic/electromagnetic coupling mechanism that does not couple the propagation of the seismic wave to the propagation of the EM wave. In particular, although all of the numerical modeling to date has concerned the first-order coupling through electrokinetics, extension to nonlinear coupling through a different mechanism is straightforward, as long as the new mechanism does not introduce coupling between the propagation parts of the problem.

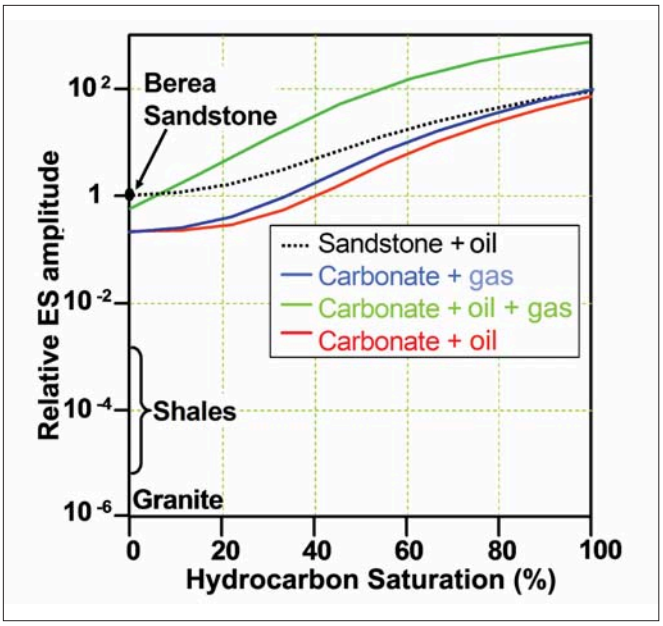

Figure 10. *Calculated ES amplitudes (relative to the amplitude for water-saturated Berea sandstone) versus hydrocarbon saturation. HC saturation alters the amplitudes by a factor of 100 or more. The saturation-dependence is large in rock containing some gas. Impermeable rock has low electrokinetic coupling.*

Summary of some model results. Figure 10 summarizes linear model calculations on a few rock types as a function of oil saturation. The models use parameters appropriate for the west Texas field test and do not attempt to address the various pore structures that characterize sandstones and carbonates.

Calculations on several thousand variations in the geology tested the trends expected for ES responses. Figure 10 shows that, for carbonates and sandstones, the hydrocarbon saturation alters the ES amplitude by a factor of 100 or more. The saturation effects are somewhat larger in carbonates than in sandstones, and gas has a larger effect than oil.

False positives for detection of hydrocarbons are unlikely for signals originating at comparable depths because the saturation effects are so large. However, competing signals can occur as a result of multiples from shallower conversions. Multiples from shallow sources have distinctive offset-dependent amplitudes that can be used to identify them. Modeling may be needed to understand the relative amplitudes of multiples when compared to deeper target signals.

Source shales, containing some mobile hydrocarbon, and sealing shales, that do not contain hydrocarbon, will have very small ES responses because their permeabilities are so low that second-order electrokinetic effects reduce the coupling amplitude. Likewise, granite, with its very small permeability, will have negligible conversion. *ES conversion requires the presence of mobile fluids.*

One important conclusion from Figure 10 is that ES is likely to be an on/off detector of hydrocarbons. The response goes through a rapid increase of one to two orders of magnitude as the saturation increases from 20 to 60%. The conversion is less sensitive to changes at low or high saturation levels. This sensitivity to hydrocarbon saturation will tend to sharpen aerial amplitude maps for delineating hydrocarbons within a particular lithology. This, of course, will occur when a portion of the reservoir has high hydrocarbon saturation and when the related large conversion amplitude exceeds the noise level.

The modeling shows that a single gas layer, one centimeter thick, can increase the ES amplitude. Stacking many layers can increase the response by several orders of magnitude over the conversion from a single layer of water-saturated rock. Inhomogeneity plays an important role. Reservoirs are electrically inhomogeneous because the hydrocarbon is not uniformly distributed. This inhomogeneity should further enhance the ES conversion and increase the contrast between aquifers and reservoirs.

The results from these layered calculations provide protocols for hydrocarbon detection in new locations. First, model the response of the subsurface assuming only aquifers are present in the predicted lithologies. Compare the results of the model calculations to the field data. ES amplitudes much larger than the predictions of the aquifer estimates suggest the presence of hydrocarbons.

Note on model limitations. There is an important distinction between ES modeling and modeling in seismology. In seismology, the seismic wavelength sets the scale of investigation. In ES, the geology sets the scale.

ES conversions occur at all locations where there are appropriate variations in rock and fluid properties. Inhomogeneities from cm to km in size can create ES conversions. The electromagnetic wavelength of the source current is larger than the size of most structures that generate ES conversions. A priori, we probably will not be able to know enough about the subsurface to predict absolute amplitudes of ES conversions ahead of the bit.

Ultimately, the value of ES surveying to hydrocarbon exploration and production rests on our ability to interpret the data. At a superficial level, the presence of a large ES signal is a clear indicator of hydrocarbon and of value without interpretation. On a more detailed level, ES gives us structural information about the location of hydrocarbons that should be of use in production.

The future of electroseismic methods, conclusions. We conclude that ES is now a viable exploration and production tool for shallow targets. Improvements in field equipment may substantially improve signal excitation to depths of several kilometers. The principal barrier we see to ES applications at greater depth concerns noise coherent with the source. Extraction of the small ES signals from random noise requires many repetitions in a stack. The remaining noise is coherent with the source. We have devised several approaches to reducing source noise, but these are untested. Substantial work also remains on higher-order conversions and their interpretation.

High-order conversions. One of us (Thompson, personal communication) investigated the possible connection between high-order conversions and the dielectric constant of moist rock. Dipolar relaxation at low frequencies and the spontaneous potential provide a mechanism for high-order ES conversion. Coupling to the macroscopic internal field of the spontaneous potential and the subsequent release of internal stress may yield ES conversion many orders of magnitude larger than the coupling between an applied field and the randomly oriented surface dipoles in electrokinetic coupling. ES coupling through the SP has the properties needed to explain the high-order ES observations. Field measurements need to confirm the predictions of this model.

Implications of high-order conversions. The existence of high-order conversions opens new lines of research in geophysics. For example, induced-polarization responses from reservoirs should be nonlinear and related to hydrocarbon saturation.

The polarizability of the SP should be observable in an active SP logging measurement where an applied field is used to modulate the SP. Modulation of the SP should carry

information about the electrochemistry at rock interfaces, the hydrocarbon saturation, and the conductivity of the brine in the pore space.

There should also be applications of nonlinear SP and ES in hydrology and archeological surveying. ES should be a sensitive indicator of nonaqueous pollutants in the near surface.

Technology improvements. At the west Texas test site, our first-generation research equipment was marginally up to the task. Experience gained from these tests suggests that many improvements in equipment and methods are possible. We anticipate that sources can be designed that will permit injection of ten times the current with better fidelity and higher frequencies. Higher-power sources will permit data collection with fewer repetitions in a stack and many source locations. Data collection at greater offsets and "roll-along" collection are feasible. Roll-along data collection may be useful in suppressing source noise.

We have made numerous studies of electrode configurations and now see ways to construct electrodes to reduce the effects of source noise and permit more rapid deployment of electrodes. New designs require smaller amounts of wire and associated equipment.

Improvements in equipment, field methods, electrode configurations, signal processing, and source power should substantially improve the S/N ratio, in environments similar to west Texas. By extrapolation from existing data, we conclude that it is feasible to excite ES conversions to depths of several kilometers. We do not anticipate that the electromagnetic skin depth will limit the application to depth. Other issues, such as near-surface noise, may be a greater problem than depth penetration.

ES data with moveout. The data reported here utilize the vertically propagating P-wave generated by the ES conversion. Improved field methods should permit data collection at far offsets from the source. Far offset data will detect P-waves with one-way moveout information that should complement seismic data.

Suggested reading. "Field tests of electroseismic hydrocarbon detection" by Thompson et al. (GEOPHYSICS, 2007). "Waveform design for electroseismic exploration" by Hornbostel and Thompson (GEOPHYSICS, 2007). "Geophysical applications of electrokinetic conversion" by Thompson and Gist (*TLE*, 1993). "Governing equations for the coupled electromagnetics and acoustics of porous media" by Pride (*Physical Review B*, 1994). "Asymptotic theory of electroseismic prospecting" by White (*Journal on Applied Mathemathics*, 2005). "Telluric currents: The natural environment and interactions with man-made systems" by Lanzerotti and Gregori (in *The Earth's Electrical Environment*, Studies in Geophysics, National Academy Press, 1986.) TLE

Acknowledgments: Application of ES and SE at the field scale has involved many talented people working over many years. These include ExxonMobil colleagues: Mark Bixby, Jim Burns, Harry Deckman, Arnold Kushnick, Max Deffenbaugh, John Dickinson, Mark Ephron, Larry Gale, Grant Gist, Greg Haake, Thomas Halsey, Eric Herbolzheimer, Chris Krohn, Arnold Kushnick, Paul McCammon, Tom Murray, Pawel Peczak, Robert Raschke, C. E. Rinehart, Warren Ross, Ben White, Denny Willen, John Wride, and Minyao Zhou, and Clint Davis of Mesa Engineering, Houston.

A. H. Thompson and John R. Sumner are no longer with ExxonMobil.

Corresponding author: athompson4@houston.rr.com